

The PIM-2 Kinase Phosphorylates BAD on Serine 112 and Reverses BAD-induced Cell Death*

Received for publication, July 22, 2003

Published, JBC Papers in Press, September 3, 2003, DOI 10.1074/jbc.M307933200

Bin Yan^{‡§¶}, Marina Zemskova^{‡§¶}, Sheldon Holder[‡], Vernon Chin[‡], Andrew Kraft^{||},
Paivi J. Koskinen^{**}, and Michael Lilly^{‡¶§§}

From the [‡]Center for Molecular Biology & Gene Therapy, the Departments of [§]Microbiology and [¶]Medicine, Loma Linda University School of Medicine, Loma Linda, California 92354, the ^{||}University of Colorado Health Sciences Center, Denver, Colorado 80262, and the ^{**}Turku Centre for Biotechnology, University of Turku/Abo Akademi, Turku 20521, Finland

Hematopoietic growth factors mediate the survival and proliferation of blood-forming cells, but the mechanisms through which these proteins produce their effects are incompletely known. Recent studies have identified the *pim* family of kinases as mediators of cytokine-dependent survival signals. Several studies have identified substrates for the *pim-1* kinase, but little is known about the other family members, *pim-2* and *pim-3*. We have investigated potential functions for the *pim-2* kinase in factor-dependent murine hematopoietic cells. We find that *pim-2* mRNA and protein expression are regulated by cytokines similarly to *pim-1*. Three PIM-2 protein isoforms are produced in cytokine-treated cells. All three forms are active kinases, and the short (PIM-2(34 kDa)) form is the most active at enhancing survival of FDCP1 cells after cytokine withdrawal. This pro-survival function involves inhibition of apoptosis and caspase activation. Enforced expression of PIM-2(34 kDa) kinase does not appear to regulate expression of BCL-2, BCL-xL, BIM, or BAX proteins. However, the kinase can phosphorylate the pro-apoptotic protein BAD on serine 112, which accounts in part for its ability to reverse Bad-induced cell death. Our results indicate that *pim-2* functions similarly to *pim-1* as a pro-survival kinase and suggest that BAD is a legitimate PIM-2 substrate.

Hematopoietic cells are dependent on peptide growth factors for survival and proliferation. The hematopoietic cytokine granulocyte-macrophage colony-stimulating factor, and the related cytokines interleukin-3 (IL-3)¹ and IL-5, can induce a spectrum of responses in target cells, including proliferation, differentiation, and prevention of apoptosis. The signaling events that regulate these several phenotypic responses are of great interest, and many mediators of these responses are being characterized.

* This work was supported by National Institutes of Health Grant R01CA45672 (to M. L.) and the Academy of Finland (to P. J. K.). The costs of publication of this article were defrayed in part by the payment of page charges. This article must therefore be hereby marked "advertisement" in accordance with 18 U.S.C. Section 1734 solely to indicate this fact.

[¶] Both authors contributed equally to this work.

^{§§} To whom correspondence should be addressed: Center for Molecular Biology & Gene Therapy, School of Medicine, Loma Linda University, 11085 Campus St., Loma Linda, CA 92354. Tel.: 909-558-8777; Fax: 909-558-0177; E-mail mlilly@som.llu.edu.

¹ The abbreviations used are: IL, interleukin; GST, glutathione S-transferase; CS, calf serum; neo, neomycin; SCF, stem cell factor; ELISA, enzyme-linked immunosorbent assay; Chaps, 3-[(3-cholamidopropyl)dimethylammonio]-1-propanesulfonic acid; Pipes, 1,4-piperazinediethanesulfonic acid; DTT, dithiothreitol; Mops, 4-morpholinepropanesulfonic acid.

Among the signaling intermediates implicated in hematopoietic cell survival is the *pim-1* serine/threonine kinase (1). *pim-1* expression is regulated by hematopoietic growth factors (2, 3). Furthermore, the kinase enhances factor-independent survival of hematopoietic cells, in part through a *bcl-2*-dependent pathway (4, 5). The *pim-1* gene product is a true oncogene, in that its enforced expression in transgenic mice leads to an increased incidence of tumors (6, 7). Potential PIM-1 substrates include proteins active in cell cycle regulation and transcription, such as Cdc25 (8), PAP-1 (9), HP1 (10), NFATc1 (11), PTP-U2S (12), and the *c-myc* transcriptional co-activator p100 (13).

pim-1 belongs to a kinase family that has three members: *pim-1* (1), *pim-2* (14), and *pim-3* (15). These related enzymes show substantial homology, but differ in their tissue expression (16). It is unknown to what extent the various family members differ in their biochemical effects. The *pim-2* gene was identified as a frequent site for retroviral insertion in experimental lymphomas, both in normal and *pim-1*-deficient mice (14). The *pim-2* gene also encodes a cytoplasmic serine threonine kinase whose expression is regulated by hematopoietic cytokines (14–17). Like the PIM-1 kinase, there are multiple isoforms of PIM-2 protein (three in the mouse and potentially two in humans) due to the use of the alternative translation start codon, CTG (18).

Functional similarity between *pim-1* and *pim-2* gene products has been inferred from studies of transgenic mice. Both *pim-1* and *pim-2* induce lymphomas alone or in synergy with *c-myc* (6, 14). Furthermore, the relatively weak phenotype associated with disruption of the *pim-1* gene (19) suggests that its functions may be largely assumed by related molecules, such as the highly homologous *pim-2* gene. Little is known, however, of the biochemical and molecular events through which the PIM-2 kinase may act. We have therefore sought to characterize the effect of PIM-2 protein in immortalized hematopoietic cells and identify potential molecular events modulated by this kinase.

Our data indicate that PIM-2 kinase inhibits apoptosis induced by various stimuli. Furthermore, we implicate phosphorylation of BAD as a possible mechanism through which the enzyme may inhibit apoptosis. These data demonstrate that enforced expression of the *pim-2* gene produces effects similar to those identified for *pim-1* in immortalized hematopoietic cells.

EXPERIMENTAL PROCEDURES

Cell Lines and Culture—The IL-3-dependent murine hematopoietic cell lines FDCP1 (obtained from Dr. Scott Boswell, Indiana University) and 32Dcl3 (obtained from Dr. Irv Bernstein, Fred Hutchinson Cancer Research Center) were used for this study. Cells were cultured in RPMI1640 medium with 10% (v/v) iron-supplemented calf serum, and 10% (v/v) medium conditioned by the WEHI-3B cell line (a convenient source of IL-3). Jurkat cells (ATCC) were grown in RPMI 1640 medium

with 10% iron-supplemented calf serum. All cells were maintained at 37 °C in 5% CO₂. HeLa, NIH3T3, and U2OS cells were maintained in McCoy's medium plus 10% iron-supplemented calf serum.

Plasmids and cDNA Clones—The cDNA for the short form of murine PIM-2 protein (PIM-2(34 kDa)) was cloned from an FDCP1 cell cDNA library by PCR, using the published sequence for primer design. The cDNAs for long (PIM-2(40 kDa)) and medium (PIM-2(38 kDa)) forms were cloned by a similar approach from a murine spleen library (Stratagene). The cDNA for kinase-inactive PIM-2 was prepared by introducing a K61A mutation into the cDNA for both short and long forms of murine PIM-2 (long or short PIM-2(K61A)), by a PCR-based technique. In each case the start codon was changed to ATG, and was preceded by an idealized Kozak sequence. All cDNAs were ligated into the mammalian expression plasmid pCDNA3 (Invitrogen), then sequenced completely to ensure the absence of unintended mutations. A mammalian expression plasmid for a GST/murine BAD chimeric protein (pEBG/Bad) was obtained from New England Biolabs, and point mutations resulting in an S112A mutation were introduced into pEBG/Bad by standard molecular techniques. A puromycin resistance plasmid (pPGK/puro) was kindly provided by Dr. Glenn Begley. A mammalian expression plasmid for human *pim-1* was prepared by subcloning the coding region from pLXSN/hpim33 (4) into plasmid pCDNA3. For bacterial expression of the recombinant enzymes, the cDNA for the short form of PIM-2 was cloned into the plasmid pET15b, as was the cDNA for the short form of PIM-1.

Transient Transfections—Transient transfection of human HeLa, U2OS, and murine NIH3T3 cells were performed in six-well plates. Near-confluent cells were transfected using 0.5–1.0 µg of each plasmid and FuGENE 6 transfection reagent, according to the manufacturer's protocol. Twelve hours later the medium was replaced with serum-free medium. After an additional 36 h of culture the cells were lysed and utilized for immunoblot analysis.

Human Jurkat T cell leukemia cells were also utilized for transient transfection assays. Mammalian expression plasmids (10 µg of each test plasmid, plus 2.5 µg of a dsRed-encoding plasmid (Clontech)) were added to 5 × 10⁶ Jurkat cells in 0.4-ml serum-free medium, followed by electroporation (Gene Pulser I; 960 microfarads and 270 V). The cells were then cultured in complete medium for 24 h and analyzed by FACS analysis for expression of the dsRed marker transgene.

Construction of Stable Cell Lines—FDCP1 and 32Dcl3 cell lines stably expressing *pim-2* constructs were prepared by electroporation. Ectopic expression of the PIM-2 isoforms was verified by immunoblotting (see below).

FDCP1 cells stably expressing *neo* or *pim-2(34 kDa)* constructs were further transfected by electroporation with pEBG/Bad and pPGK/puro to produce additional cell lines. Puromycin-resistant clones were examined for GST/BAD expression by immunoblotting. Positive clones were then utilized for biochemical and cell growth experiments.

Cell Survival and Apoptosis Assays—For enumeration of surviving cells, trypan blue-negative cells in 0.9 mm³ of suspension were counted in triplicate with a hemocytometer. Apoptosis was detected by an annexin V binding assay, using commercially available reagents (OncoGene Sciences). Cells were stained with both an annexin V-fluorescein isothiocyanate conjugate and propidium iodide. The proportion of cells that were fluorescein isothiocyanate high but PI low was taken to be the early apoptotic population. Populations were quantitated by two-color flow cytometry, using a BD Biosciences FACScan instrument.

Anti-PIM-2 Monoclonal Antibody—A monoclonal antibody to murine PIM-2 protein was prepared as follows. BALB/c mice were immunized with recombinant murine PIM-2(40 kDa) protein. The antigen was produced in *Escherichia coli* as a 6-His-tagged fusion protein, utilizing the bacterial expression plasmid pET15b (Novagen). The recombinant protein was purified by affinity chromatography on a cobalt resin (Talon, Clontech) and was shown to consist of a single band on Coomassie Blue-stained SDS-PAGE gel. Following fusion and selection, clones were screened by ELISA assay. Positive wells contained antibodies that reacted with recombinant murine PIM-2 protein but not recombinant human or murine PIM-1 protein. Positive clones were screened further by immunoblotting and immunoprecipitation. One clone, 1D12 (IgG₁), was selected for its ability to detect murine PIM-2 protein by both of these methods.

Northern Blotting—mRNAs for *pim-1* and *pim-2* were detected by Northern blotting. 30 µg of total RNA were resolved on formaldehyde-agarose gels, transferred to nylon membranes, and probed with ³²P-labeled cDNA probes. For *pim-2* detection the probe consisted of a full-length murine *pim-2* cDNA. The *pim-1* probe consisted of an EcoRI-BamHI fragment of the cDNA excised from pLXSN/hpim33 (4). A 600-bp fragment of the chicken β-actin cDNA was utilized as the control

probe. Probes were nick-labeled with [³²P]dCTP using a commercially available kit (Bio-Rad).

Western Blotting—Cells were collected, washed in phosphate-buffered saline, and lysed in either 1% Triton lysis buffer (20 mM Tris, pH 7.5, 100 mM NaCl, 5 mM EDTA, 1% Triton X-100, 10 mM NaF, 1 mM Na₃VO₄, 20 µg/ml leupeptin, 10 µg/ml pepstatin, 10 µg/ml aprotinin) by vortexing, or in Chaps lysis buffer (50 mM Pipes/NaOH, pH 6.5, 2 mM EDTA, 1.0% Chaps, 5 mM DTT, 20 µg/ml leupeptin, 10 µg/ml pepstatin, 10 µg/ml aprotinin, 1 mM phenylmethylsulfonyl fluoride) by three freeze/thaw cycles. Lysate protein was then measured (BCA method; Pierce), and lysates were mixed with an equal volume of 2× Laemmli buffer. Equal amounts of total protein were added to each well for electrophoresis in 10% SDS-polyacrylamide gels and then transferred to polyvinylidene fluoride membranes (Millipore Corp.). Membranes were blocked, then incubated with primary antibodies, followed by incubation with horseradish peroxidase-linked secondary antibodies. Antibody-antigen complexes were detected using chemiluminescence (Pierce). The following primary antibodies were used: anti-PIM-2 (described above), anti-BCL-2 (Santa Cruz Biotechnology), anti-BCL-xL (Santa Cruz Biotechnology), anti-BAX (Santa Cruz Biotechnology), anti-BIM (Chemicon), anti-procaspase 3 (Santa Cruz Biotechnology), anti-active caspase 3 (Cell Signaling), goat anti-BAD (Santa Cruz Biotechnology; for transfected BAD proteins), mouse monoclonal anti-BAD (BD Transduction Laboratories; for endogenous BAD), and anti-phospho-Ser112 BAD, anti-phospho-Ser136 BAD, and anti-phospho-Ser155 BAD (Cell Signaling).

In Vitro Kinase Assay—HeLa cells were transiently transfected with an expression plasmid for PIM-2(34 kDa) protein. Expressing cells were harvested then lysed in IP lysis buffer (1 mM DTT, 10 mM NaF, 1 mM Na₃VO₄, 20 mM Tris, pH 7.5, 100 mM NaCl, 5 mM EDTA, 1% Triton X-100, 1 mM phenylmethylsulfonyl fluoride, 20 µg/ml leupeptin, 10 µg/ml pepstatin, 10 µg/ml aprotinin). Alternatively, PIM-2 proteins were produced by *in vitro* translation, using pCDNA3-based plasmids and a commercial kit (TnT T7 Quick, Promega), followed by dilution of the reaction products in IP lysis buffer. In either case PIM-2 was immunoprecipitated with anti-PIM-2 antibodies. Immune complexes were washed with IP lysis buffer once, high salt IP buffer (IP buffer with 500 mM NaCl) twice, low salt IP buffer (IP buffer without NaCl) once, and then twice with PK wash buffer (20 mM MOPS, pH 7.4, 10 mM β-glycerophosphate, and 1 mM DTT). Reactions were done in 20-µl volumes, in kinase assay buffer (20 mM MOPS, pH 7.4, NaCl 150 mM, 12.5 mM MgCl₂, 1 mM MnCl₂, 1 mM EGTA, 10 mM β-glycerophosphate, 1 mM DTT, 0.5 µM protein kinase inhibitor peptide (PKI), 10 µM ATP) supplemented with 1 µl of [γ-³²P]ATP (PerkinElmer Life Sciences) and 1 µg of GST-BAD recombinant protein as a substrate. Reactions were incubated at 30 °C for 30 min. Kinase reactions were then diluted to 1 ml with stop buffer (50 mM Tris-HCl, pH 8.0, 0.5 M NaCl, 10 mM EDTA, 10 mM EGTA, 10% glycerol), and the supernatants were transferred to 25 µl of GST-agarose bead in a new tube. Samples were incubated with rocking at 4 °C for 1 h. Then beads were washed with stop buffer for three times. The GST-BAD retained on the beads was then dissolved in Laemmli buffer and resolved by SDS-PAGE. The dried gels were visualized by autoradiography. Alternately kinase reactions were performed in buffer with 100 µM “cold” ATP but no radioactive ATP. In this case the phosphorylated substrate protein was analyzed by immunoblotting with anti-phospho-BAD antibodies.

The PIM-2 kinase assay was also performed in ELISA format. Wells of a polystyrene 96-well plate were coated with GST-BAD protein. Following blocking with bovine serum albumin, recombinant 6-His-PIM-1(33 kDa) or 6-His-PIM-2(34 kDa) protein was added in the above kinase buffer with cold ATP. The kinase reaction was allowed to proceed for 1 h at 30 °C. Wells were then washed extensively. Phosphorylated substrate was then detected by addition of anti-phospho-BAD S112 antibody (1:1000) for 1 h at room temperature. The second antibody was a peroxidase-coupled anti-mouse IgG. Color development utilized Turbo-TMB reagents (Pierce). Reactions were read on an ELISA plate reader at 450 nm.

For estimation of enzyme kinetics with the ELISA kinase assay, time-course experiments were performed in ELISA plates coated with different concentrations of substrate (0.5–2.0 µg/well). Enzyme concentrations were 100 ng of kinase per reaction. Enzyme protein concentration was measured with the BCA assay method (Pierce). Initial velocity (V_i) was estimated by the term, $d(A_{450})/dt$, measured over the first 12 min of the reaction. Subsequent time points were also measured to ensure that the reaction rate was linear for at least 18 min. Two separate experiments, utilizing separate enzyme preparations, were performed, and the results were examined by Lineweaver-Burk analysis. In addition the Michaelis-Menten data were analyzed by non-linear

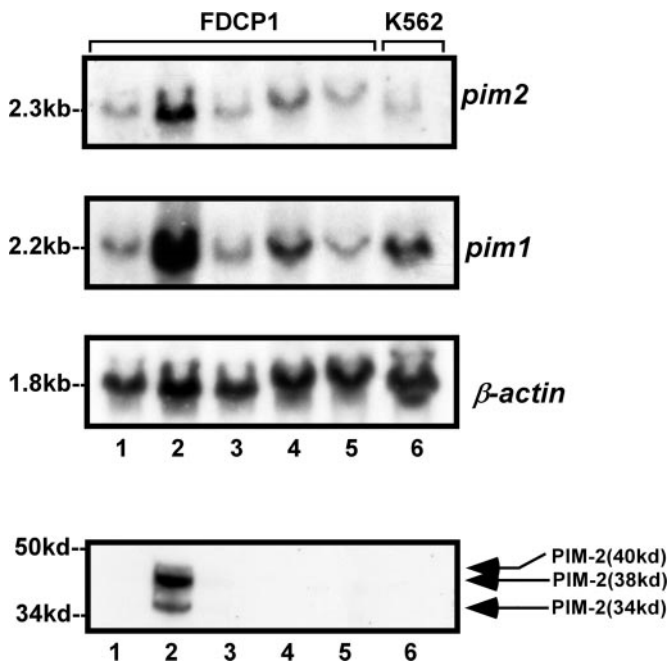


FIG. 1. Northern, Western blots of *pim-2* expression. *Top panel*, Northern blot of cytokine-treated FDCP1 cells or untreated K562 cells, probed with murine *pim-2* cDNA probe. *Second panel*, Northern blot probed with human *pim-1* cDNA probe. *Third panel*, Northern blot probed with chicken β -actin cDNA probe. *Bottom panel*, immunoblot of FDCP1 or K562 cells, blotted with anti-PIM-2 monoclonal antibody. All cells were deprived of IL-3 for 4 h, then cultured with cytokines as follows: *lane 1*, no cytokine \times 2 h; *lane 2*, rmIL-3 10 ng/ml \times 2 h; *lane 3*, rhIL-1 α 10 ng/ml \times 2 h; *lane 4*, rmIL-4 10 ng/ml \times 2 h; *lane 5*, rmSCF 100 ng/ml \times 2 h.

regression, using the program PRISM (GraphPad Software), to obtain the estimates of V_{max} and T_m .

RESULTS

*Expression of *pim-2* mRNA and Protein Is Regulated by Cytokines in a Similar Pattern to That of *pim-1**—The ability of *pim-2* to functionally compensate for the lack of *pim-1* (14) suggests also that the expression of these two genes might be regulated in a similar fashion. To test this possibility, we cultured FDCP1 cells without IL-3 for 4 h and then stimulated them with a variety of cytokines for an additional 2 h. Northern blotting showed that both *pim-1* and *pim-2* mRNAs were induced by IL-3 and to a lesser extent by IL-4 (Fig. 1). By contrast, stem cell factor and IL-1 α were unable to induce expression of either message.

To determine if PIM-2 protein levels correlated with *pim-2* mRNA expression, we developed a specific anti-PIM-2 monoclonal antibody. The 1D12 antibody identified PIM-2 protein with no detection of PIM-1 in immunoblots of transiently transfected HeLa cells (Fig. 2). FDCP1 cells expressed three PIM-2 forms, as expected (14), with the intermediate form being most abundant. PIM-2 protein levels closely paralleled the changes in mRNA (Fig. 1). FDCP1 cells deprived of cytokine had little PIM-2. IL-3 treatment induced a marked increase in the kinase protein. Prolonged exposure of the blot showed that IL-4 minimally induced expression of PIM-2, but stem cell factor and IL-1 α failed to promote expression of the kinase (not shown).

*Transfection of Murine Hematopoietic Cells with *pim-2* Expression Plasmids*—To identify potential biological effects mediated by *pim-2*, we expressed the various isoforms, as well as an inactive kinase, in two factor-dependent murine hematopoietic cells, FDCP1 and 32Dcl3. In each case enforced expression resulted in a marked increase in the corresponding isoform protein (Fig. 3A; 32D cell data not shown). Levels of the PIM-

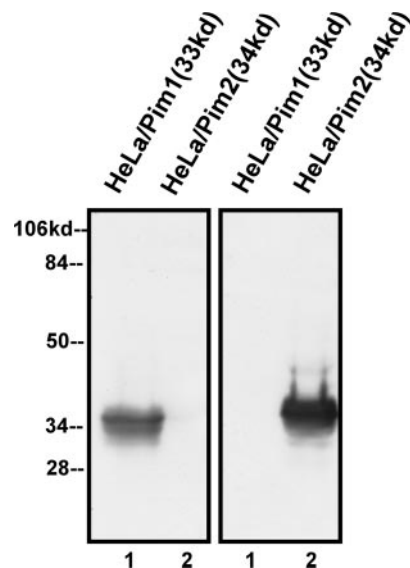


FIG. 2. Immunoblot of HeLa cell lysates. HeLa cells were transiently transfected with mammalian expression plasmids for either human *pim-1* (33 kDa) (*lane 1*) or murine *pim-2* (34 kDa) (*lane 2*). Lysates were subjected to immunoblotting with either monoclonal anti-PIM-1 antibody (clone 19F7; *left panel*) or monoclonal anti-PIM-2 (clone 1D12; *right panel*).

2(38 kDa) protein in both cell lines were somewhat lower than for the other two forms. Expression of the kinase-dead long PIM-2(K61A) mutant was also detected. Expression of the transgene products did not decrease after IL-3 withdrawal in the FDCP1-derived cells or in 32Dcl3-based cell lines.

The half-life of the expressed transgene proteins in stably transfected FDCP1 cells was measured after cycloheximide blockade of new protein synthesis (Fig. 3, B and C). The PIM-2(38 kDa) protein exhibited an extremely short half-life (10–15 min), whereas the PIM-2(40 kDa) was somewhat longer (about 30 min). In contrast, PIM-2(34 kDa) had a half-life in excess of 60 min. Endogenous PIM-2 proteins were not seen due to the short exposure times for the films.

PIM-2 Enhances Survival of Hematopoietic Cells after IL-3 Withdrawal or Doxorubicin Treatment—Both FD/neo and 32D/neo cells died in the absence of IL-3. Cells expressing *pim-2* transgenes also died, but at a slower rate (Fig. 4; 32D cell data not shown) with some viable cells persisting for several days. The three isoforms of PIM-2 showed different survival effects. The shortest form (PIM-2(34 kDa)) was the most active isoform at inhibiting cell death, resulting in little change in cell number for up to 70 h of cytokine deprivation. However, the long and medium forms of PIM-2 were less active at delaying cell death. As expected, a kinase-dead K61A mutant did not promote factor-independent survival and actually appeared to enhance death during the initial observation period. In this respect the K61A mutant acts similarly to a dominant-negative PIM-1 protein, which also increases cell death during cytokine withdrawal (5).

The *pim-1* kinase has been implicated in resistance to genotoxic stresses such as ionizing radiation and cytotoxic drugs (20). We found that enforced expression of the active PIM-2(34 kDa) kinase also enhanced resistance to doxorubicin in FDCP1 cells, leading to a 2-fold increase in the ID₅₀ for that agent (data not shown), compared with FD/neo cells.

PIM-2 Inhibits Apoptosis and the Activation of Caspase 3 Associated with IL-3 Deprivation—Cell death in hematopoietic cells following cytokine withdrawal is thought to result from apoptosis, or programmed cell death. We have previously demonstrated that the *pim-1* kinase inhibits the onset of apoptosis

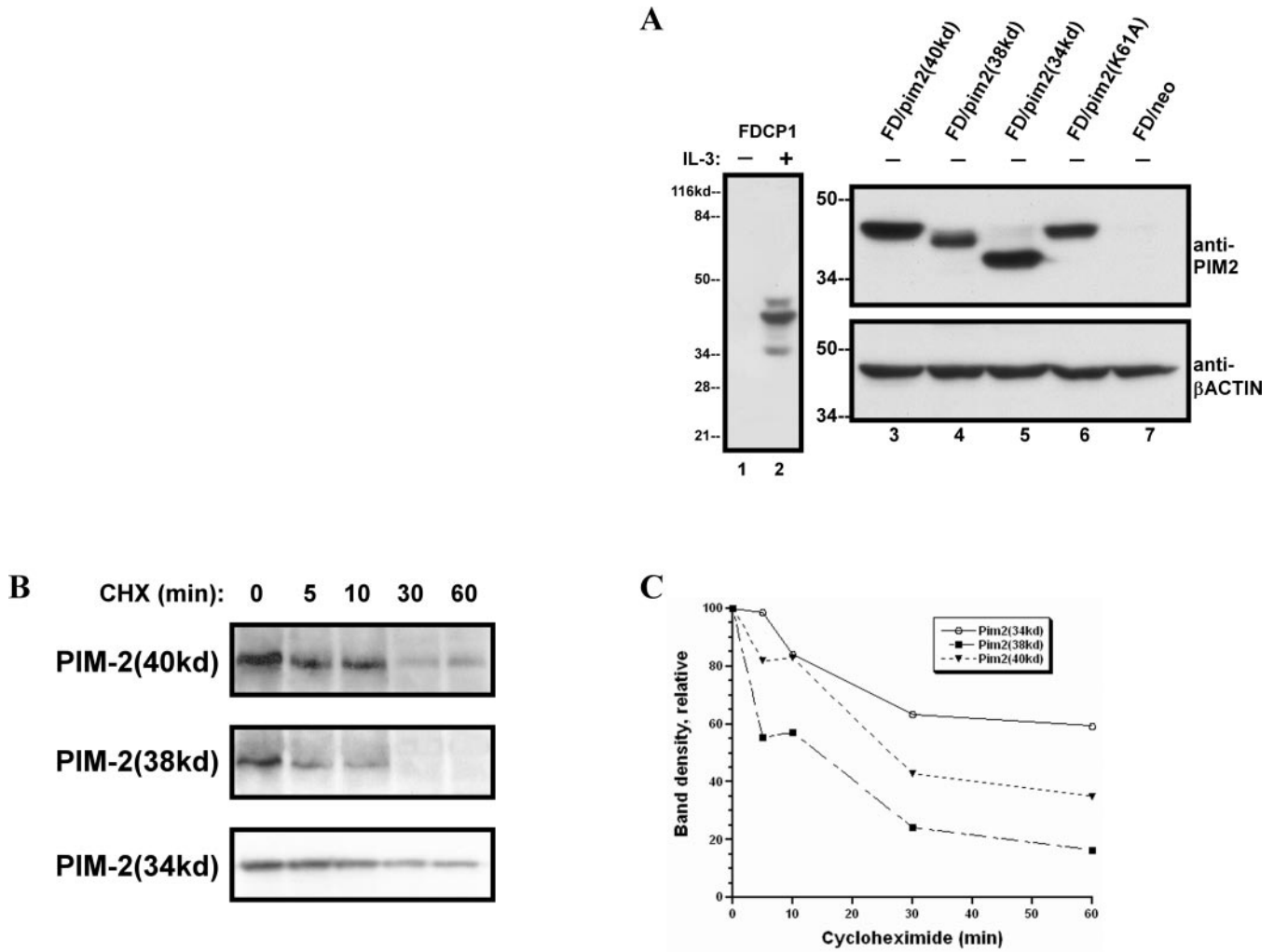


FIG. 3. Immunoblots of pim-2 transgene expression in stably-transfected FDCP1 cells. *A*, transgene expression. *Lane 1*, untransfected FDCP1 cells cultured without IL-3 × 6 h; *lane 2*, untransfected cells maintained in IL-3; *lanes 3–7*, transfected FDCP1 cells growing in IL-3 were treated with cycloheximide (20 μg/ml) for the indicated periods. Equal numbers of cells were then lysed and analyzed for PIM-2 proteins by immunoblotting with anti-PIM-2 monoclonal antibody. *C*, decay curves for PIM-2 proteins. Video densitometry was performed on bands of immunoblots in *B*.

following IL-3 removal in FDCP1 cells (4). Thus we questioned if the survival effects of PIM-2 protein resulted from decreased apoptosis. Because the greatest pro-survival effects were associated with enforced expression of the PIM-2(34 kDa) protein, subsequent studies focused on this kinase isoform. Apoptotic cells were measured by flow cytometry in FD/neo and FD/Pim-2(34 kDa) cells following IL-3 withdrawal. FD/neo cells had an increased proportion of cells within which were annexin V-positive and propidium iodide-negative, consistent with an increase in apoptosis (Fig. 5A).

A mitochondria-mediated mechanism of caspase activation is involved in apoptosis induced by genotoxic drugs and growth factor withdrawal. We have examined whether overexpression of PIM-2 can regulate the activation of caspase 3 (Fig. 5B). IL-3 deprivation led to a decrease in the 34-kDa caspase 3 precursor in FD/neo cells, accompanied by a concomitant increase in the 17-kDa active fragment. In contrast, cleavage of caspase 3 precursor was remarkably inhibited by the overexpression of PIM-2 in FD/Pim-2(34 kDa) cells. These data demonstrate that *pim-2* prevents cells from undergoing apoptosis by inhibiting caspase 3 activation.

PIM-2 Phosphorylates BAD Both in Vitro and in Vivo and Inhibits Apoptotic Effect of BAD—To study the mechanism of how *pim-2* inhibits caspase 3 activation, we examined its effects on the expression or activity of several members of the

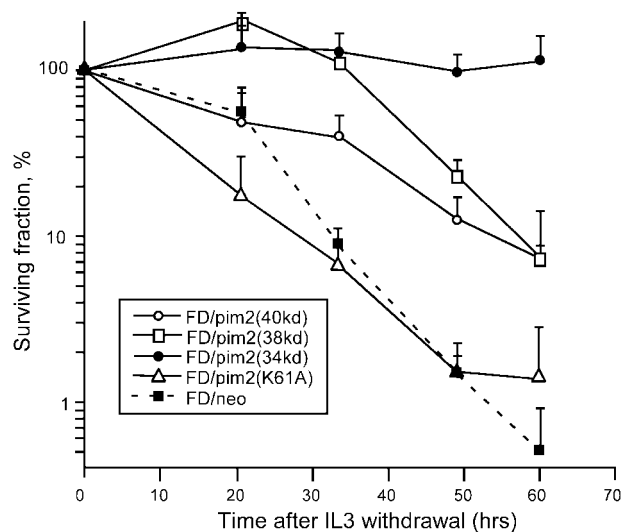


FIG. 4. Survival of FDCP1 cells stably transfected with *pim-2*. Pools (at least two clones) of FDCP1 cells expressing the three forms of PIM-2, a kinase-inactive form of the long PIM-2 protein (*pim2(K61A)*), or *neo*, were washed and cultured without IL-3. At the indicated times surviving cells were enumerated by Trypan Blue exclusion. Each point represents the mean ± S.D. of triplicate determinations from one of three similar experiments.

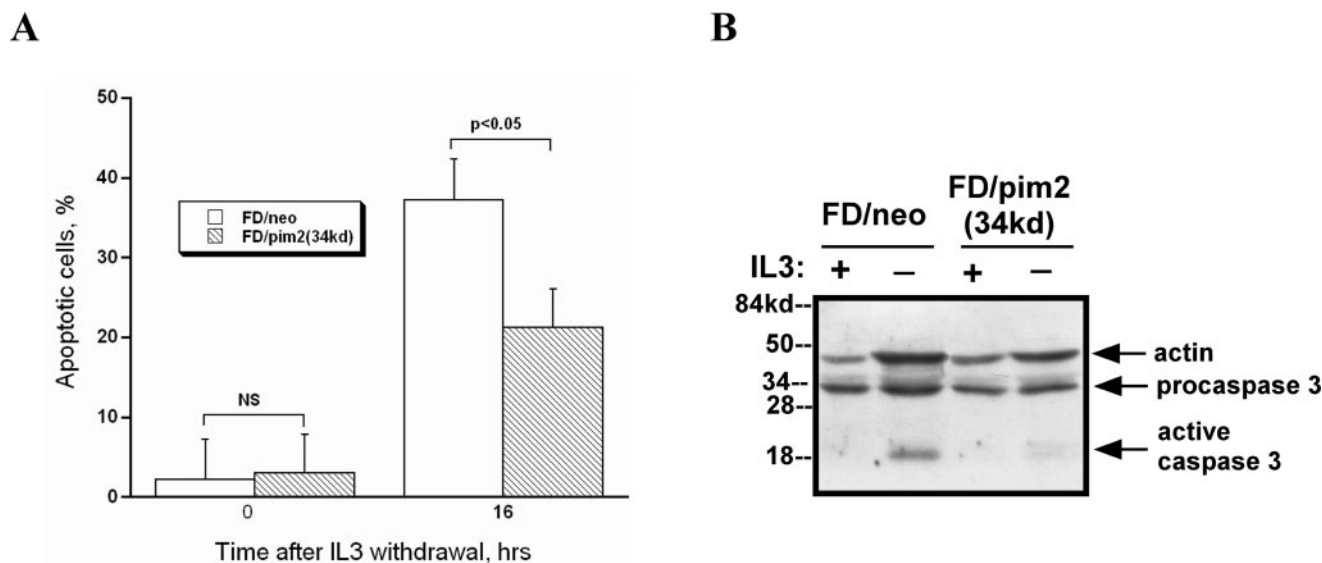


FIG. 5. **Apoptosis in FD/neo, FD/Pim-2(34 kDa) cells following IL-3 withdrawal.** *A*, apoptosis assay. Cells were cultured without cytokine for the indicated time then subjected to flow cytometry analysis to detected apoptotic cells (annexin V high; propidium iodide low). Bars indicate the mean \pm S.E. for three independent experiments (each performed in triplicate). *B*, immunoblot to detect procaspase 3 and activated caspase 3 following IL-3 withdrawal. FD/neo and FD/Pim2(34 kDa) cells were washed free of IL-3 then cultured without cytokine for 16 h. Cells were then lysed in CHAPS buffer and analyzed by immunoblotting with the indicated antibodies. Antibodies were utilized sequentially, beginning with anti-active caspase 3 and finishing with anti- β -actin. The blot was washed and reblocked between antibody probes.

BCL-2 family of survival proteins. FD/neo and FD/Pim-2(34 kDa) cells were examined by immunoblotting after culturing them in the presence or absence of IL-3. Neither IL-3 withdrawal nor enforced expression of *pim-2* led to changes in expression of BCL-2 or BAX. By contrast, IL-3 withdrawal was associated with decreased expression of BCL-xL and increased expression of BIM, but PIM-2 did not affect their expression any further (data not shown).

We have previously seen that the PIM-1 protein can antagonize the effects of BAX protein expression, independently of *bcl-2* expression (5). This suggested that PIM-1 could regulate the activity of other pro-apoptotic BCL-2 family proteins, such as BAD (5). Indeed we have seen direct evidence that PIM-1 kinase can phosphorylate BAD.² We therefore asked if the PIM-2 kinase could phosphorylate, and thereby inactivate the BAD protein, as well. IL-3 removal leads to rapid dephosphorylation of BAD, and onset of apoptosis in some factor-dependent hematopoietic cells (21). The phosphorylation consensus sequences for *pim* kinases are similar to those of AKT and cAMP-dependent (protein kinase A) kinases (22). Because these kinases can phosphorylate BAD, it seemed possible that PIM-2 could do so as well.

PIM-2 proteins were purified by immunoprecipitation from U2OS cells transfected with expression plasmids for either wild-type or kinase inactive PIM-2(34 kDa) proteins. The enzymes were then assayed in an immunocomplex kinase assay for their ability to phosphorylate recombinant GST-BAD protein. Anti-PIM-2 immunoprecipitates from wild-type kinase transfectants were able to phosphorylate GST-BAD, whereas anti-prostate-specific antibody immunoprecipitates (isotype-matched negative control antibody) failed to do so (Fig. 6A). Recombinant GST protein alone was not phosphorylated by the immunoprecipitated kinase. To characterize the reaction further, we subjected PIM-2-phosphorylated GST-BAD protein to immunoblotting with anti-phospho-BAD antibodies (Fig. 6B). GST-BAD protein phosphorylated by wild-type PIM-2(34 kDa) protein reacted strongly with antibodies recognizing BAD phos-

phorylated on serine 112. Anti-PIM-2 immunoprecipitates from cells transfected with a plasmid encoding a kinase-dead short PIM-2(K61A) could only minimally phosphorylate the substrate, probably due to small amounts of other BAD kinases coprecipitating with PIM-2. Immunoprecipitates containing a kinase-inactive long form of PIM-2 were similarly inactive (data not shown). PIM-2 appears to selectively phosphorylate GST-BAD on serine 112, because the phosphorylated substrate did not react with antibodies specific for serine 136 or serine 155 phosphorylation.

Because the PIM-2 isoforms differed in their ability to support survival of cytokine-deprived FD/neo cells, we directly determined their relative kinase activity. Proteins for the three PIM-2 isoforms were expressed by *in vitro* translation then purified by immunoprecipitation. When used in an *in vitro* kinase reaction, all were able to phosphorylate GST-BAD on serine 112. The kinase activity of the 40-kDa form toward that substrate was about 22% lower than that of the 38-kDa form, a significant difference ($p = 0.03$ for no difference). Not surprisingly, the K61A mutant 34-kDa protein had no detectable kinase activity, again suggesting that the minimal activity seen in panel B was due to coprecipitating kinases. The kinase-dead long (40-kDa) form also lacked detectable ability to phosphorylate BAD (data not shown).

We have previously noted that PIM-1 protein can phosphorylate BAD.² To compare the relative efficiency of the two kinases for the same substrate, we prepared 6-His-PIM-2(34 kDa) protein along with 6-His-PIM-1(33 kDa). The freshly prepared kinases were utilized immediately in an ELISA-formatted kinase reaction with GST-BAD as the substrate. The recombinant PIM-2 protein phosphorylated GST-BAD in the ELISA format. Time-course experiments showed that the initial reaction rate typically was linear for at least 18 min (Fig. 7A). As expected, with longer incubation the reaction rate declined. A series of time-course experiments was performed, with differing quantity of substrate in the wells. The initial reaction rate (measured over the first 12 min) was then compared with substrate concentration by Lineweaver-Burk analysis (Fig. 7B). The resulting linear plot confirmed that the Pim-2 enzyme demonstrated kinetics consistent with Michael-

² T. L. T. Aho, J. Sandholm, K. J. Peltola, H. P. Mankonen, M. Lilly, and P. J. Koskinen, manuscript submitted.

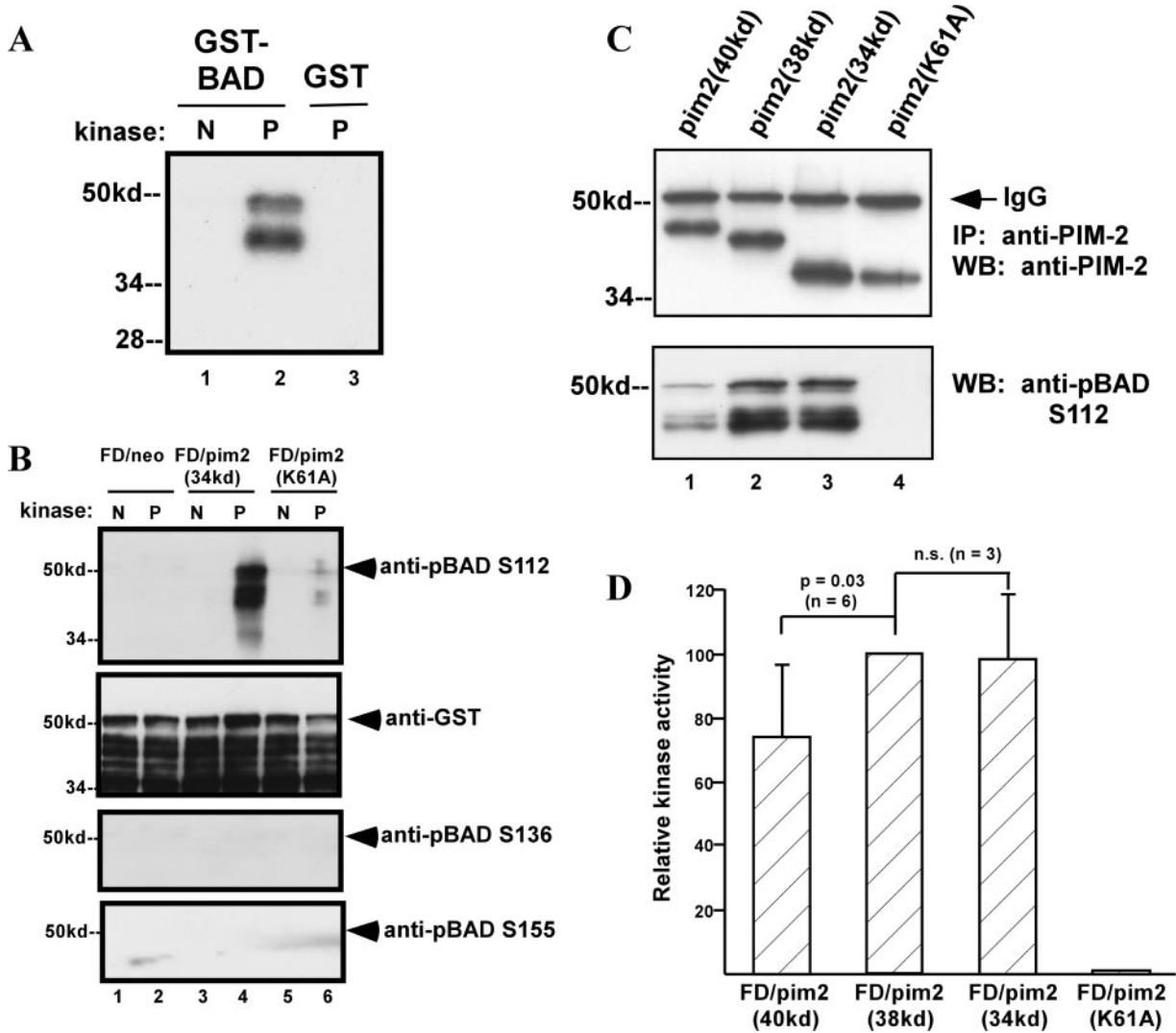


FIG. 6. *In vitro* phosphorylation of GST-BAD by PIM-2. A, autoradiograph of ³²P-labeled GST-BAD. The PIM-2 was immunoprecipitated from transiently transfected U2OS cells by anti-PIM-2 antibody (P) or an isotype-matched control antibody (N), then mixed with either recombinant GST or GST-BAD proteins. After radioactive *in vitro* kinase reaction, the substrates were separated by SDS-PAGE and visualized by autoradiography. The lower band represents degradation products and aborted proteins. B, immunoblot of GST-BAD phosphorylated *in vitro* by PIM-2. Anti-PIM-2 immunoprecipitates (lanes 2, 4, and 6) or irrelevant immunoprecipitates (lanes 1, 3, and 5) were used to phosphorylate GST-BAD. Substrate was then immunoblotted with anti-phospho-Bad or anti-GST antibodies. C, comparative activity of PIM-2 proteins as BAD kinases. The 34-, 38-, and 40-kDa PIM-2 proteins, or the short PIM-2(K61A) protein were produced by *in vitro* translation, and purified by immunoprecipitation. The resulting enzymes were used for an *in vitro* kinase reaction, and the phosphorylated GST-BAD substrate protein was then detected by immunoblotting with an anti-phospho-BAD S112 antibody. D, quantitative analysis of GST-BAD phosphorylation by PIM-2 proteins. For each experiment anti-phospho-BAD(S112) band density was normalized by comparing it to the PIM-2 protein band density. In each experiment the normalized density for GST-BAD phosphorylated by PIM-2(38 kDa) was assigned an arbitrary value of 100. This served as an internal reference to compare the normalized phospho-BAD band densities (and hence kinase activities) of the other enzymes. Finally, the results of three to six experimental comparisons were averaged and presented as mean ± S.D. Relative kinase activity of PIM-2(40 kDa) versus PIM-2(38 kDa) (six comparisons), and of PIM-2(34 kDa) versus PIM-2(38 kDa) (three comparisons), were analyzed by paired *t* tests.

lis-Menten predictions. It was also apparent from the Lineweaver-Burk plot that the lines for PIM-2 and PIM-1 were parallel, and therefore the slopes (K_m/V_{max}) were equal. This suggests that PIM-1 and PIM-2 may be equivalent kinases for phosphorylating GST-BAD protein. True V_{max} values could not be calculated from the ELISA-derived data, because the reaction rate is described in terms of change of color ($d(A_{450})/dt$) rather than the more traditional millimoles/liter/min. The apparent V_{max} and T_m values can be used only as relative indices to compare PIM-1 and PIM-2 but not for comparisons with values for other kinases, as recorded in the literature. Non-linear regression analysis of the Michaelis-Menten data showed no significant differences in the estimated V_{max} and T_m for the two kinases in either of the two experiments (data not shown).

We next examined the phosphorylation of BAD by PIM-2 *in*

vivo, using a transient transfection system. U2OS and 3T3 cells were transfected with expression plasmids for PIM-2(34 kDa) and GST-BAD, alone or in combination (Fig. 8). In the presence of PIM-2, GST-BAD was heavily phosphorylated on serine 112 in both cell lines. Interestingly, in U2OS cells there was additional phosphorylation of serine 136 and serine 155. In contrast, in 3T3 cells only serine 112 was phosphorylated in the presence of PIM-2. Expression of the *pim-2* transgene product was much higher in the U2OS cells, however.

We also stably co-transfected FD/neo and FD/Pim-2(34 kDa) cells with a GST-BAD mammalian expression construct and a puromycin resistance plasmid. A GST-BAD fusion protein was expressed, because we were unable to isolate stable lines expressing wild-type BAD proteins. Presumably the GST-BAD fusion protein has somewhat less death-promoting activity than the wild-type BAD protein, allowing stably expressing

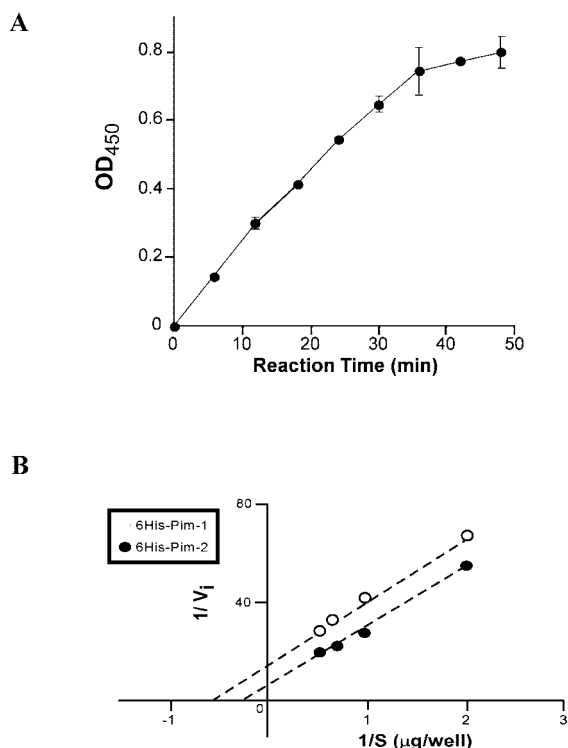


FIG. 7. Phosphorylation of GST-BAD by PIM-2: ELISA-based kinase assay. *A*, time course of phosphorylation. A 96-well plate was coated with 1.5 μg/well GST-BAD overnight, then the plate was blocked with bovine serum albumin. 100 ng of 6-His-PIM-2 protein was added in 100 μl of kinase buffer, 10 μM ATP, and the reaction was allowed to proceed for 1 h at 30 °C. The reactants were then aspirated, and the reaction was stopped by washing the wells with 10 mM EDTA in Tris-buffered saline. Phosphorylated substrate was detected by developing the plate with successive incubations with anti-phospho-BAD(S112) antibody, goat anti-mouse IgG-peroxidase, and TMP-based color reagents. Each point is the mean ± S.D. of triplicate determinations from a typical experiment. *B*, Lineweaver-Burk analysis of enzyme reaction time course data. Kinetic measurements were obtained as in *A*, but with substrate concentrations ranging from 0.5 to 2.0 μg/well. V_i is $d(A_{450})/dt$ obtained from first 12 min of enzyme activity time course. 6-His-PIM-2 and 6-His-PIM-1 were used at 100 ng/well.

clones to be identified. Puromycin-resistant clones were examined for expression of GST-BAD by immunoblotting with an anti-BAD antibody. Several clones of FD/Pim-2(34 kDa)/Bad and FD/neo/Bad cells were isolated, and three clones of each were pooled. Enforced expression of GST-BAD in FD/neo cells enhanced death, compared with FD/neo/puro cells (Fig. 9). However, enforced expression of PIM-2 protein was able to overcome the exaggerated death effect of GST-BAD.

We therefore examined the extent of GST-BAD phosphorylation in the stable transfectants after IL-3 withdrawal (Fig. 10A). FD/neo/Bad cells grown in IL-3 demonstrated phosphorylation of GST-Bad on serine 112. Phosphorylation decreased after withdrawal of IL-3. The FD/Pim-2(34 kDa)/Bad cells had markedly increased phosphorylation of GST-BAD, which changed little after IL-3 withdrawal. Phosphorylation of BAD on serine 136 or serine 155 was not detected under these conditions.

Finally we sought to determine if ambient amounts of PIM-2 could phosphorylate endogenous BAD (Fig. 10B). FDCP1 cells stably expressing either *neo*, PIM-2(34 kDa) protein, or long PIM-2(K61A) protein were deprived of IL-3 for 10 h. Whole cell lysates were then used for immunoblotting. The endogenous BAD protein was detected in all samples. In three independent experiments, BAD showed slight but reproducible phosphorylation on serine 112 in FD/neo cells. FD/Pim-2(34 kDa) had

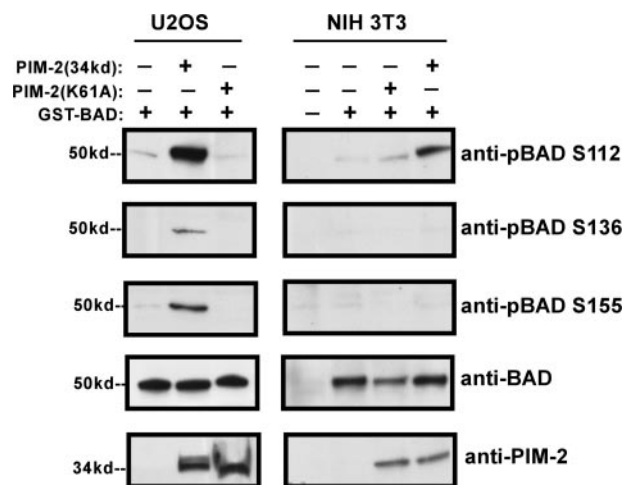


FIG. 8. Phosphorylation of GST-BAD by PIM-2 in transiently transfected cells. U2OS or NIH3T3 cells were transiently transfected with the indicated plasmids (0.5 μg of each) in 60-mm plates. pCDNA3 plasmid was added to ensure that each transfection contained the same total amount of plasmid DNA. 48 h after transfection, cells were lysed and subjected to immunoblot analysis with the indicated antibodies. Twenty micrograms of lysate protein was loaded per lane.

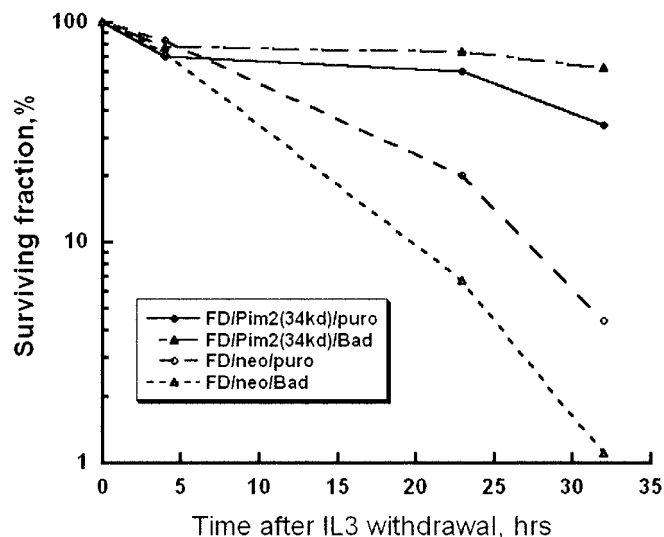


FIG. 9. Survival of FDCP1 cells expressing GST-BAD and PIM-2 after IL-3 withdrawal. Pools of stable transfectants (three clones each) were cultured without IL-3. At the indicated times, surviving cells were enumerated by Trypan Blue exclusion. Each point represents the mean of triplicate determinations from one of two similar experiments.

greatly increased phosphorylation of endogenous BAD. In contrast, cells with kinase-dead PIM-2 had no detectable phosphorylation of endogenous BAD.

PIM-2 Inhibits BAD-induced Cell Death in Part through Phosphorylation of BAD on Serine 112—To determine if phosphorylation of BAD on serine 112 played a role in the ability of PIM-2 to inhibit BAD-induced cell death, we sought to co-express PIM-2 and a mutant GST-BAD that could not be phosphorylated on serine 112. However, we were unable to isolate FDCP1-based cell lines with these characteristics. The GST-BAD(S112A) proteins were invariably truncated (data not shown). We therefore chose to transiently co-express PIM-2 and GST-BAD or GST-BAD(S112A) in Jurkat T-cells (Fig. 11). This cell line was used because it can be transfected more efficiently than FDCP1 and has previously been used for studies of BAD kinases. Cells were also transfected with an expression plasmid for the fluorescent protein DsRed (Clontech) to

FIG. 10. Phosphorylation of BAD proteins by PIM-2 in stably transfected FD/neo cells. *A*, phosphorylation of GST-BAD in FD/neo/Bad and FD/Pim2(34 kDa)/Bad cells. Pools of stable transfectants (three clones each) were cultured with or without cytokine for 6 h, as indicated. Whole cell lysates were then prepared, and 50 μg of lysate protein was loaded on each lane. Blots were then probed with the indicated antibodies. *B*, phosphorylation of endogenous BAD by exogenous, endogenous PIM-2. FD/neo cells, stably transfected with *neo*, PIM-2(34 kDa), or kinase-dead long PIM-2(K61A), were deprived of IL-3 and cultured for 10 h. Whole cell lysates were then prepared and used for immunoblotting as indicated. 250 μg of whole cell lysate was used for each lane of the blot.

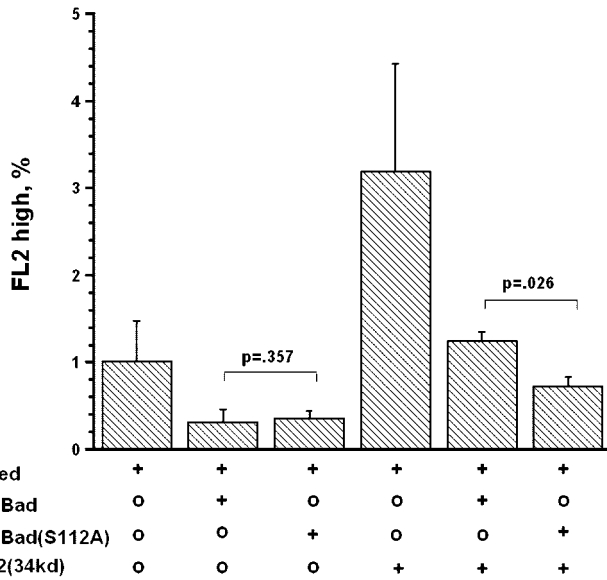
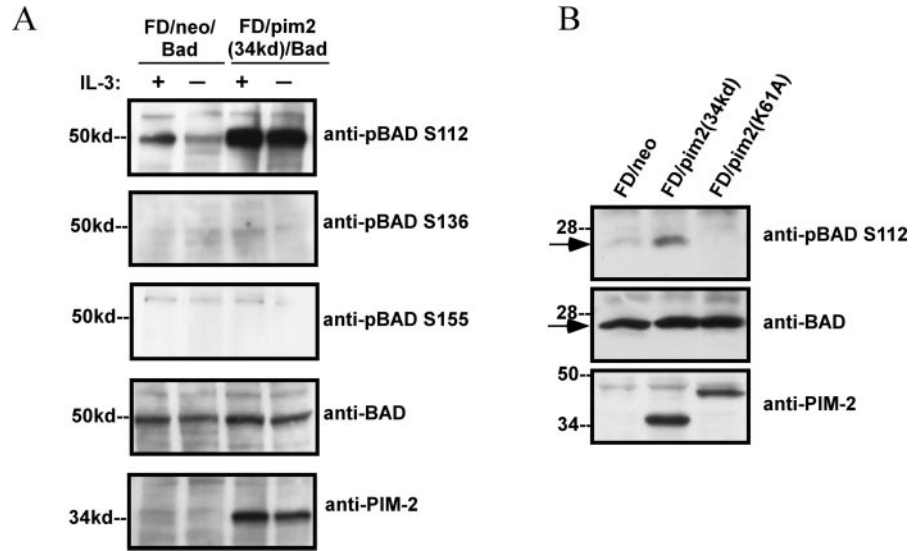


FIG. 11. Dependence on S112 phosphorylation for reversal of GST-BAD-induced death by PIM-2. Jurkat cells were transiently transfected with the indicated plasmid. pCDNA3 plasmid was included as needed to ensure that each transfection contained the same amount of total plasmid DNA. 24 h later they were analyzed by FACS analysis for expression of the transfection marker protein dsRed. Results are normalized (mean percentage of FL2-high cells from transfections with dsRed plasmid alone = 1.0). For each experiment, measurements were made in triplicate, and averaged. Each bar represents the mean ± S.E. from three independent experiments.

mark transfected cells. Twenty-four hours later the transfected cells were analyzed by flow cytometry. Between 1.35 and 4.29% of cells transfected with a *DsRed* plasmid alone were highly red fluorescent. Adding the GST-BAD expression plasmids markedly reduced the number of red fluorescent cells, demonstrating that the two GST-BAD proteins equally induced cell death in the transfected cells. In contrast, co-transfection with a *pim-2* expression plasmid increased the number of red fluorescent cells, reflecting the ability of the kinase to promote survival of the transfected population. Cells were also transfected simultaneously with plasmids encoding PIM-2(34 kDa) and GST-BAD or GST-BAD(S112A), along with the *DsRed* expression plasmid. Enforced expression of PIM-2(34 kDa) protein was markedly better at preventing cell death in the presence of GST-BAD protein, compared with its ability to reverse the effects of the GST-BAD(S112A) protein (*p* = 0.026 for no dif-

ference). These data demonstrate that antagonism of GST-BAD by PIM-2(34 kDa) depends at least in part on the ability of the kinase to phosphorylate GST-BAD on serine 112.

DISCUSSION

IL-3, granulocyte-macrophage colony-stimulating factor, and related growth factors induce proliferation and differentiation of hematopoietic cells and protect them from apoptosis. We have shown that this family of cytokines selectively induces the expression of *pim* family kinases in hematopoietic cells. The *pim* kinases show tissue-specific expression (16). Few studies have examined functional or biochemical redundancy within the family, however. *pim-1* and *pim-2* appear to be regulated similarly (2, 3, 17). Because these kinases share functional activities (6, 14, 17), it is likely that they may also act through similar biochemical pathways. A recent report documented that both PIM-1 and PIM-2 can phosphorylate the SOCS-1 protein (23). With this exception, however, no studies have identified potential PIM-2 substrates. We now report that PIM-2 can phosphorylate and inactivate BAD and that its efficiency as a BAD kinase resembles that of PIM-1. Although we cannot conclude that PIM-1 and PIM-2 are equally efficient for all substrates, these data do suggest that any unique roles for the different kinases may result from their variable tissue expression (16).

Three PIM-2 isoforms are apparent in FD/neo and 32Dcl3 cells. The endogenous PIM-2(38 kDa) protein is more abundant than the other isoforms. This parallels the results reported from *in vitro* translation of the *pim-2* cDNA (14). In contrast, when expressed as a transgene, PIM-2(38 kDa) was the least abundant form. Under these conditions protein expression likely reflects in part kinase stability, with the 38-kDa form of PIM-2 being less stable, and consequently expressed at a lower level. In aggregate these data suggest that transcriptional and translational regulation may both play an important role in the relative levels of the various isoforms in the natural state. In the *pim-2* mRNA sequence, the translational start site AUG for PIM-2(34 kDa) is preceded by UCCUCC, whereas the alternative start codon CUG for PIM-2(40 kDa) is preceded by UUGGGG. For PIM-2(38 kDa) the start codon is preceded by UCCACC. Compared with the usual Kozak sequence GCC(G/A)CC, the start codons for PIM-2(40 kDa) and PIM-2(34 kDa) are preceded by poor Kozak consensus sequences. This observation, combined with the fact that the CUG codon for PIM-2(38 kDa) is in a more favorable translational context, may help to explain the levels of endogenous PIM-2 isoforms.

The biological and biochemical effects of these three isoforms differ as well. When the pure proteins were examined with an *in vitro* kinase assay, the 34- and 38-kDa forms showed similar activity, whereas the 40-kDa was noticeably and reproducibly deficient. As expected the K61A mutant enzymes were inactive. It is not clear why the 40-kDa form is less active than the shorter enzymes. Possibly the additional sequences in the 40-kDa form constitute an autoinhibitory sequence. Because the 40- and 34-kDa forms were expressed at similar levels in the stably transfected FDCP1 cells, it is likely that the intrinsic differences in kinase activity accounts for the impaired survival effect of the longer kinase. The 34- and 38-kDa PIM-2 proteins showed similar ability to phosphorylate BAD *in vitro*, yet the 38-kDa enzyme was slightly less active at prolonging survival in cytokine-deprived FDCP1 cells. In this situation, the lower level of expression of PIM-2(38 kDa) in the stably transfected cells, compared with that of PIM-2(34 kDa), may account for the superior survival effect of the latter kinase.

The mechanisms through which *pim-2* acts to promote cell survival and inhibit programmed cell death have not been previously characterized. Our previous studies of the *pim-1* kinase documented the involvement of *bcl-2* family members (5). Because of the strong homology between the two kinases, they may act through similar biochemical processes. We have previously observed that the PIM-1 kinase can phosphorylate BAD² and report here that the PIM-2 kinase can act similarly. PIM-2 kinase, immunoprecipitated from transfected cells, was able to directly phosphorylate a GST-BAD substrate *in vitro*, on serine 112. In contrast, in U2OS cells transiently transfected with both *pim-2* and *gst-bad* expression plasmids, the substrate was phosphorylated on serine 112, serine 136, and serine 155. These additional phosphorylations may be the result of PIM-2 activating other kinases, rather than a direct effect of PIM-2 protein itself. Certainly the *in vitro* kinase reactions, which are known to encourage promiscuous phosphorylations, did not show detectable serine 136 or serine 155 phospho-BAD. In addition we have seen that co-transfection of a dominant-negative *akt* construct, along with *pim-2* and *gst-bad* plasmids, markedly decreases the serine 136 phosphorylation of the substrate (data not shown). We feel that this potential transactivation of AKT (and serine 155 kinases) by PIM-2 is unlikely to be of physiological significance. No serine 136 or serine 155 phosphorylation was seen in an NIH3T3 transient transfection system, in which expressed levels of the transgenes were lower than those seen in U2OS cells. Furthermore we found no evidence of serine 136 or serine 155 phosphorylation in stable FDCP1 cells co-expressing the two cDNAs. Thus it appears that serine 112 is the preferred phosphorylation site on BAD, for the PIM-2 kinase. Minimal phosphorylation at other sites likely does not mediate a significant part of the PIM-2 effect.

Serine 112 of BAD appears to be the preferred phosphate acceptor site for kinase reactions involving both PIM-1² and PIM-2. The sequence surrounding serine 112 includes several positively charged amino acids, but only distantly resemble a consensus PIM phosphorylation site (22). Several other known PIM-1 substrates also have atypical phosphorylation sites; thus it is not clear how comprehensive the described consensus sequences are for predicting PIM substrates. PIM-2 now joins several other enzymes as known kinases for BAD (serine 112). These include protein kinase A (24), JNK1 kinase (25), p90/RSK kinase (26), and PAK1 kinase (27). It is not clear if ambient levels of all of these other kinases can phosphorylate endogenous BAD protein. Because our data show that enforced expression of a kinase-inactive PIM-2 protein both decreases phosphorylation of endogenous BAD and shortens cell survival relative to that of *neo*-expressing cells (which retain partial

BAD phosphorylation), we can identify BAD as a legitimate substrate for PIM-2 kinase expressed at ambient levels, as well as when overexpressed in a test system.

Enforced expression of PIM-2 was able to overcome the death-promoting effects of GST-BAD in both stable and transiently transfected cells. However, our inability to isolate FDCP1 stably co-expressing PIM-2 and a mutant GST-BAD(S112A) suggested that phosphorylation of GST-BAD by the PIM-2 kinase on serine 112 was important for this reversal. This was directly confirmed in the transient transfection experiments. Enforced expression of either GST-BAD or GST-BAD(S112A) similarly reduced the number of successfully transfected cells, whereas PIM-2 increased marker transgene expression. Co-expression of the cDNAs reversed the death-enhancing effects of both of the GST-BAD constructs. However, reversal of the GST-BAD-induced death was much more efficient than correction of the GST-BAD(S112A) toxicity. While confirming the need of PIM-2 to phosphorylate BAD on serine 112 for maximal effects, these data also suggest that other molecular targets may be involved. Indeed some studies question the role of BAD in survival of cytokine-deprived hematopoietic cells (28, 29). The temporal correlation between decreased phosphorylation of endogenous BAD in the presence of enforced expression of kinase-dead PIM-2, and enhanced cell death (Fig. 4, 10), suggest that BAD plays some role in survival of these cells, and that it likely mediates part of the survival effect of PIM-2. We anticipate, however, that *pim* kinases regulate a variety of survival pathways. Recently, PIM-1 has been found to phosphorylate and regulate the activity of the p21/Waf1 protein, a key mediator of p53-dependent programmed cell death (30). We have performed a large number of genetic screens for PIM substrates and partners and have found many candidates, several of which can be implicated in survival responses. Thus it is likely that many additional interactions between PIM family kinases and survival pathways will be identified in the future.

REFERENCES

1. Selten, G., Cuypers, H. T., Boelens, W., Robanus-Maandag, E., Verbeek, J., Domen, J., van Beveren, C., and Berns, A. (1986) *Cell* **46**, 603–611
2. Dautry, F., Weil, D., Yu, J., and Dautry-Varsat, A. (1988) *J. Biol. Chem.* **263**, 17615–17620
3. Lilly, M., Le, T., Holland, P., and Hendrickson, S. L. (1992) *Oncogene* **7**, 727–732
4. Lilly, M., and Kraft, A. (1997) *Cancer Res.* **57**, 5348–5355
5. Lilly, M., Sandholm, J., Cooper, J. J., Koskinen, P., and Kraft, A. (1999) *Oncogene* **18**, 4022–4031
6. van Lohuizen, J., Verbeek, S., Krimpenfort, P., Domen, J., Saris, C., Radzskiewicz, T., and Berns, A. (1989) *Cell* **56**, 673–682
7. Breuer, M., Wientjens, E., Verbeek, S., Slebos, R., and Berns, A. (1991) *Cancer Res.* **51**, 958–963
8. Mochizuk, I. T., Kitanaka, C., Noguchi, K., Muramatsu, T., Asia, A., and Kuchino, Y. (1999) *J. Biol. Chem.* **274**, 18659–18666
9. Maita, H., Harada, Y., Nagakubo, D., Kitaura, H., Ikeda, M., Tamai, K., Takahashi, K., Ariga, H., and Iguchi-Ariga, S. M. (2000) *Eur. J. Biochem.* **267**, 5168–5178
10. Koike, N., Maita, H., Taira, T., Ariga, H., and Iguchi-Ariga, S. M. (2000) *FEBS Lett.* **467**, 17–21
11. Rainio, E. M., Sandholm, J., and Koskinen, P. J. (2002) *J. Immunol.* **168**, 1524–1527
12. Wang, Z. P., Bhattacharya, N., Meyer, M. K. E., Seimiya, H., Tsuruo, T., Tonani, J. A., and Magnuson, N. S. (2001) *Arch. Biochem. Biophys.* **390**, 9–18
13. Levenson, J. D., Koskinen, P. J., Orrico, P. C., Rainio, E. M., Jalkanen, K. J., Dash, A. B., Eisenman, R. N., and Ness, S. A. (1998) *Mol. Cell.* **2**, 417–425
14. van der Lugt, N. M., Domen, J., Verhoeven, E., Linders, K., van der Gulden, H., Allen, J., and Berns, A. (1995) *EMBO J.* **14**, 2536–2544
15. Feldman, J. D., Vician, L., Crispino, M., Tocco, G., Marcheselli, V. L., Bazan, N. G., Baudry M., and Herschman, H. R. (1998) *J. Biol. Chem.* **273**, 16535–16543
16. Eichmann, A., Yuan, L., Breant, C., Alitalo, K., and Koskinen, P. J. (2000) *Oncogene* **19**, 1215–1224
17. Allen, J. D., Verhoeven, E., Domen, J., vanderValk, M., and Berns, A. (1997) *Oncogene* **15**, 1133–1141
18. Saris, C. J., Domen, J., and Berns, A. (1991) *EMBO J.* **10**, 655–664
19. Laird, P. W., van der Lugt, N. M., Clarke, A., Domen, J., Linders, K., McWhir, J., Berns, A., and Hooper, M. (1993) *Nucleic Acids Res.* **21**, 4750–4755
20. Pircher, T. J., Zhao, S. Q., Geiger, J. N., Joneja, B., and Wojchowski, D. M. (2000) *Oncogene* **19**, 3684–3692

21. Salomoni, P., Condorelli, F., Sweeney, S. M., and Calabretta, B. (2000) *Blood* **96**, 676–684
22. Friedmann, M., Nissen M. S., Hoover, D. S., Reeves, R., and Magnuson, N. S. (1992) *Arch. Biochem. Biophys.* **298**, 594–601
23. Chen, X. P., Losman, J. A., Cowan, S., Donahue, E., Fay, S., Vuong, B. Q., Nawijn, M. C., Capece, D., Cohan, V. L., and Rothman, P. (2002) *Proc. Natl. Acad. Sci. U. S. A.* **99**, 2175–2180
24. Harada, H. H., Becknell, B., Wilm, M., Mann, M., Huang, L. J. S., Taylor, S. S., Scott, J. D., and Korsmeyer, S. J. (1999) *Mol. Cell* **3**, 413–422
25. She, Q. B., Ma, W. Y., Zhong, S. P., and Dong, Z. G. (2002) *J. Biol. Chem.* **277**, 24039–24048
26. Bertolotto, C., Maulon, L., Filippa, N., Baier, G., and Auberger, P. (2000) *J. Biol. Chem.* **275**, 37246–37250
27. Schurmann, A., Mooney, A. F., Sanders, L. C., Sells, M. A., Wang, H. G., Reed, J. C., and Bokoch, G. M. (2000) *Mol. Cell. Biol.* **20**, 453–461
28. Hinton, H. J., and Welham, M. J. (1999) *J. Immunol.* **162**, 7002–7009
29. Neshat, M. S., Raitano, A. B., Wang, H. G., Reed, J. C., and Sawyers, C. L. (2000) *Mol. Cell. Biol.* **20**, 1179–1186
30. Wang, Z., Bhattacharya, N., Mixter, P. F., Wei, W., Sedivy, J., and Magnuson, N. S. (2002) *Biochim. Biophys. Acta* **1593**, 45–55